Proceedings of the 21st ICSMGE, Vienna, Austria, 14 – 19 June 2026. Pistrol, Adam & Schweiger (eds.)
Published by: ÖGG, Austrian Society for Geomechanics, Salzburg, Austria, ISBN 978-3-9503898-4-5
https://doi.org/10.53243/ICSMGE2026-2377

Horizontal Loading Test and Analytical Study for Soil-Cement Composite Piles

Shohei Koga
Civil Engineering Construction Division, Obayashi Corporation, Tokyo, Japan, koga.shohei@obayashi.co.jp

Koji Watanabe
Department of Civil Engineering, Faculty of Engineering, Aichi Institute of Technology, Toyota, Japan

ABSTRACT: There are several pile construction methods that use small construction machinery suitable for narrow urban spaces and areas with low overhead clearance. The top-drive boring hole method, which has a machine height of 4.5 m, is often used. However, there are many cases where architectural limitations and existing structures interfere with even these construction machines. The boring hole pile method can handle narrow spaces and low overhead clearances better than the top-drive boring hole method. However, because the boring hole pile method is a direct circulation method, mud cakes easily form on the hole walls, and slime tends to accumulate at the pile tip. Such challenges related to the construction method, bearing capacity, and settlement require solutions to facilitate pile construction in narrow urban spaces. Therefore, a method for soil-cement composite pile construction was developed that uses a compact mechanical agitator for pile foundations of lightweight structures. The construction machine is a mechanical agitator with an attached vibration mechanism and improved drilling capacity. The aim of this study is to investigate the use of soil-cement composite piles, which have been conventionally designed as temporary structures, in permanent structures. To evaluate the lateral resistance of soil-cement composite piles, a full-scale horizontal loading test was performed on piles of two diameters. In addition, numerical analyses were performed to simulate full-scale horizontal loading tests, with the friction between the pile and the ground and the adhesion between the soil-cement and H-section steel pile as parameters. The behavior of soil-cement composite piles with horizontal forces was simulated by elasto-plastic finite element method analysis using joint elements modeling the friction between the pile and the ground and the adhesion between the soil-cement and H-section steel pile.

KEYWORDS: Soil-Cement Composite Pile, Lateral Resistance, In Situ Full-Scale Loading Test, Numerical Analysis.

1 INTRODUCTION

There are several pile construction methods that are suitable for construction in narrow urban spaces and areas with low overhead clearance; for example, the top-drive boring hole (TBH) method and the boring hole (BH) pile method. However, the TBH method has a machine height of 4.5 m and architectural limitations and existing structures can still interfere with these construction machines. In contrast, the BH pile method can handle narrow spaces and low overhead clearances better than the TBH method. Because the BH pile method is a direct circulation method, mud cakes easily form on the hole walls, and slime tends to accumulate at the pile tip, lowering the bearing capacity of the piles and making subsidence of the pile more likely to occur. Such challenges related to the construction method, bearing capacity, and settlement require solutions to facilitate pile construction in narrow urban spaces. Furthermore, the effects of noise and industrial waste on the surrounding environment must be considered.

Soil-cement composite piles, which are fabricated using a method for H-section steel pile construction combined with soil-cement ground improvement, use a compact mechanical agitator for pile foundations of lightweight structures (Koga et al., 2022). The mechanical agitator (i.e., e-column construction method) with an attached vibrating mechanism and improved drilling capacity that can be used for pile construction in narrow spaces where construction is usually difficult (Figure 1). This method does not require drilling up to a fixed depth as in the pre-boring pile construction method. Instead, soil is agitated along with the cement milk at the original position. Therefore, the amount of construction sludge for the pile is greatly reduced.

In this study, we examine the application of soil-cement composite piles, which have been conventionally designed as temporary structures (Railway Technical Research Institute, 2001), and permanent structures. There have been studies of the lateral resistance and failure of piles with soil-cement (Kitaura et al., 2014), but there are no studies on piles with H-section steel inserted into the soil-cement. To evaluate the lateral resistance of the soil-cement composite piles, a full-scale horizontal loading test was performed on soil-cement composite piles of two diameters. In addition, numerical analyses were performed to simulate full-scale horizontal load tests with the friction between the pile and the ground and the adhesion between the soil-cement and the H-section steel pile as the parameters. Modeling to evaluate the lateral resistance of soil-cement composite piles suitably is discussed.

Figure 1. Construction machine for soil-cement composite piles.

2 IN SITU FULL-SCALE HORIZONTAL LOAD TEST

Figure 2 shows the soil profile and test piles. The test ground was composed of loam and tuffaceous clay up to about ground level (GL) −5.0 m and sandy silt, medium sand, and fine sand below that. Table 1 presents the specifications of the test piles. The test piles were constructed with pile diameters of 600 and 800 mm for Types 1 and 2, respectively. The static load test was carried out based on the standards of the Japanese Geotechnical Society “Methods for Lateral Load Test of Piles” (Japanese Geotechnical Society, 2010). A stepwise multi-cycle loading system was used with a new load holding period of 2 min, hysteretic load holding duration of 2 min, and zero load holding

duration of 14 min. The measured items were the pile head load, pile head displacements, and strain of the H-section steel. The strain gauge was a uniaxial two wire system attached to the inside of the flange with adhesive. The strain of the H-section steel was measured at intervals of 600 mm up to GL −4.2 m where the horizontal force was dominant, and at intervals of 1.2 m below that. The arrangement of the test piles and reaction piles is shown in Figure 3. Two test piles and three reaction piles were constructed. Similar to the test piles, three reaction piles were also constructed as H-section steel piles with soil-cement by the same construction method as the test piles. The distance between the test piles and the reaction piles were set based on the influence range as described in the standard (Japanese Geotechnical Society, 2010). The distances were 3D = 1800 and 2400 mm, where D is the pile diameter defined as the soil-cement diameter. Before the horizontal load test, these two test piles were subjected to the compression load test and tensile load test. These two test piles were given the required curing period, which is described in the standard (Japanese Geotechnical Society, 2010), after the compression load test and tensile load test. After the compression load test and tensile load test, the pile heads were checked to ensure that there was no damage.

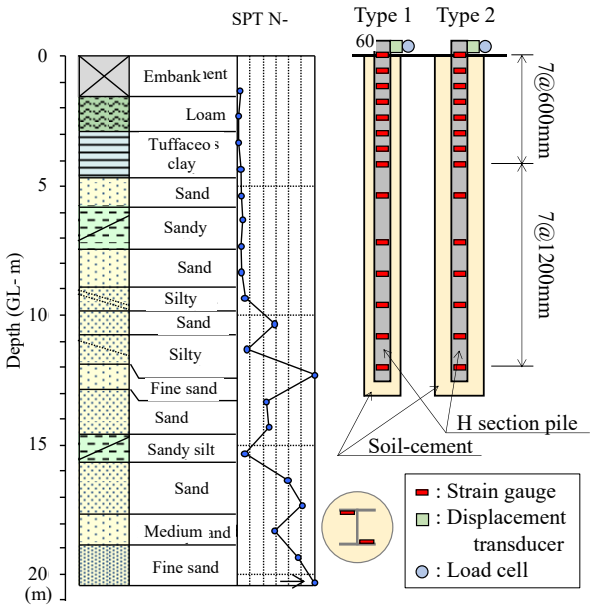

Figure 2. Soil profile and test piles.

Table 1. Specifications of test piles

Pile ID	Pile diameter (mm)	Pile length (m)	UCS of soil-cement (kN/m^2)
Type 1	600	14.0	1,000
Type 2	800	14.0	1,000

USC, unconfined compression strength (kN/m^2)

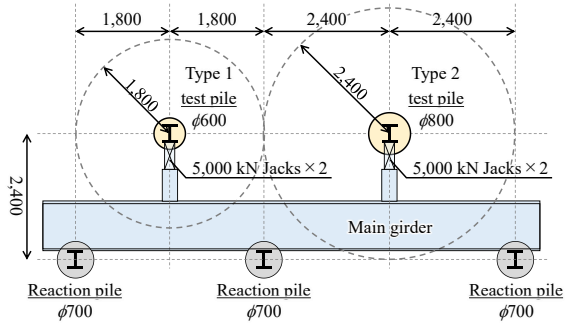

Figure 3. Arrangement of test piles and reaction piles.

3 NUMERICAL ANALYSIS

To simulate the results of the in situ full-scale horizontal loading test, numerical analysis using an elasto-plastic finite element method was performed. In this analysis, the H-section steel was modeled as elastic, and the soil-cement and ground were modeled as elasto-plastic using Mohr–Coulomb failure criterion. Figure 4 shows the analytical model. The test piles were modeled according to Table 1, and the ground shown in Figure 2 was modeled as a total of six soil layers, divided into two major categories: sandy soil and clay soil. The size of the analytical model was determined based on the area of influence under horizontal loading, as shown in the standard (Japanese Geotechnical Society, 2010).

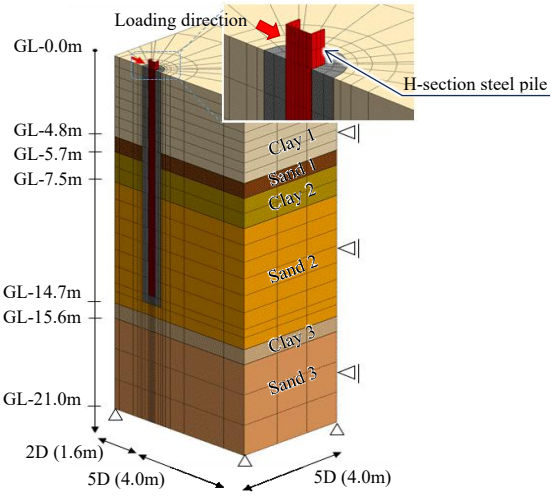

Figure 4. Analytical model (Type 2).

To evaluate the suitability of modeling methods for simulating the behavior of the soil-cement composite piles under the horizontal force, the H-section steel was modeled using a common method involving three-dimensional solid elements and as well as one-dimensional beam elements. The beam element shown in Figure 5 (a) is given the sectional stiffness of the H-section steel pile to simulate the bending of the H-section steel. Then, a rigid plate element is used to connect the nodes of the solid soil-cement element and the H-section steel element to transmit forces.

To simulate the slippage between the H-section steel and the soil-cement element and between the soil-cement element and the ground, 1.0 mm thin solid elements were added at each boundary (Figure 5 (b)). These thin solid elements reduce the adhesion and internal friction angles that contribute to shear behavior to simulate slippage. The deformation modulus and Poisson's ratio, which contribute to the deformation, were equal to those of the ground and soil-cement.

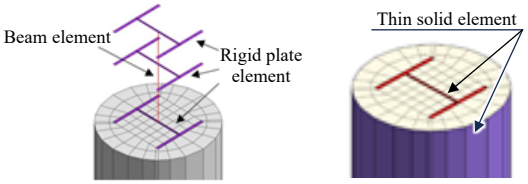

(a) Beam element model for H-section steel

(b) Thin solid element for slippage

Figure 5. Details of the analytical model.

Table 2 shows the input constants. The ground parameters in for the analysis were calculated using the estimating equations given in the standard (Railway Technical Research Institute,

2012) using only the N values obtained from the standard penetration tests. Equations (1) to (3) are the equations for calculating the deformation modulus for sands and clay shown in the standard (Railway Technical Research Institute, 2012). The deformation coefficients for sand and clay were calculated using equations Equation (2) and (3), respectively.

$$E_d = \rho_{gE} E_N / \gamma_{gE} \quad (1)$$

$$E_N = 2000N \quad (2)$$

$$E_N = 4000N \quad (3)$$

E_d: Design deformation modulus used to calculate the coefficient of subgrade reaction for foundations (kN/m^2). E_N: Standard penetration test value of the deformation modulus (kN/m^2). ρ_{gE}: Modified coefficient of ground for the deformation modulus (ρ_{gE} = 1.0). γ_{gE}: Coefficient of soil investigation for deformation modulus (γ_{gE} = 1.4). N: Standard penetration test N value. Equations (4) and (5) are the estimated equations for calculating the internal friction angle of sand and the cohesion of clay in the standard (Railway Technical Research Institute, 2012).

$$\varphi = 1.85\left(\frac{N}{\sigma_v'/100 + 0.7}\right)^{0.6} + 26 \quad (4)$$

$$c = q_u/2 \quad (5)$$

ϕ: Internal friction angle of sand (°). σ_v': Effective overburden pressure at the corresponding depth identified during the soil investigation (kN/m^2). c: Cohesion (kN/m^2). q_u: Unconfined compression strength (kN/m^2). E_s: Young's modulus of steel (kN/m^2). The unconfined compression strength of the clay was calculated by Equation (6) (Japanese Society of Soil Mechanics and Foundation Engineering, 1982).

$$q_u = N/6 \times 100 \quad (6)$$

Table 2. Input parameters

	E_d, Es (kN/m^2)	ν	γ (kN/m^3)	c (kN/m^2)	ϕ (°)
Steel	206×10^6	0.30	76.9	-	-
Soil-cement	100,000	0.30	20.0	500.0	0.5
Clay 1	4,706	0.45	16.0	16.7	0.5
Sand 1	5,000	0.32	18.0	0.5	29.2
Clay 2	9,412	0.45	16.0	24.5	0.5
Sand 2	35,000	0.32	18.0	0.5	33.7
Clay 3	14,118	0.45	16.0	36.8	0.5
Sand 3	75,000	0.32	18.0	0.5	36.4
Thin solid Clay 1	4,706	0.45	16.0	5.0	0.5
Thin solid Sand 1	5,000	0.32	18.0	0.5	5.0
Thin solid Clay 2	9,412	0.45	16.0	5.0	0.5
Thin solid Sand 2	35,000	0.32	18.0	0.5	5.0
Thin solid Soil-cement	100,000	0.30	18.0	10.0	0.5

Table 3 shows the analysis cases. The cases that simulated the Type 1 test pile with a pile diameter of 600 mm and the Type 2 test pile with a pile diameter of 800 mm were Cases 1 and 2, respectively. The bottom of the analytical model was fixed, and the outer surface was fixed in the horizontal direction and free only in the vertical direction. The analysis for initial stresses with the dead weight was carried out first, followed by stepwise loading analysis. The maximum load was determined to be 280 kN in Case 1 and 360 kN in Case 2, corresponding to the loading steps of the in situ full-scale horizontal loading test, and the loads were increased in steps of 20 kN each. GTS NX analysis software (MIDAS) was used for the analysis.

Table 3. Analytical cases

	Modeling type of H-section steel	Thin solid element	Pile diameter (mm)
Case 1-1	Solid	off	600
Case 1-2	Beam	off	600
Case 1-3	Solid	on	600
Case 1-4	Beam	on	600
Case 2-1	Solid	off	800
Case 2-2	Beam	off	800
Case 2-3	Solid	on	800
Case 2-4	Beam	on	800

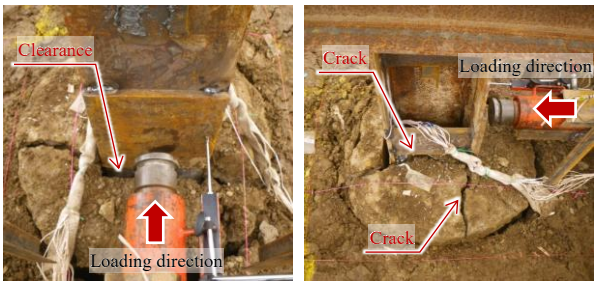

(a) From the front in the loading direction

(b) From the side in the loading direction

Figure 6. Photographs of a test pile after the horizontal loading test

4 RESULTS OF IN SITU FULL-SCALE HORIZONTAL LOADING TEST AND NUMERICAL ANALYSIS

4.1 *Appearance after horizontal loading test*

Figure 6 shows photographs of a test pile after the in situ full-scale horizontal loading test. There was a clearance of about 30 mm between the back of the H-section steel in the loading direction and the soil-cement. There were cracks developing from the tip of the flange of the H-section steel to the outer edge of the soil-cement, and cracks connecting the flange tips of the H-section steel had developed. The clearance and cracks were observed in Type 1 and 2 test piles after loading tests. The results suggest that as the maximum horizontal load was reached, tensile forces at the boundary between the soil-cement and the H-section steel caused separation, which in turn induced shear failure at the tip of the H-section steel flange.

4.2 *Relationships between horizontal load and displacement at ground level*

Figure 7 shows the relationship between horizontal load and displacement at ground level for full-scale horizontal loading tests. The results for Cases 1-2 and 1-4 and Cases 2-2 and 2-4 are also shown to determine the effect of thin solid elements on the simulation of slippage between the H-section steel and soil-cement and between the soil-cement and ground. Cases 1-2 and 2-2 do not have thin solid elements, whereas Cases 1-4 and 2-4 do. The results of the loading test showed that from the beginning of loading to displacement at ground surface level of about 60 mm, the horizontal load values at the same displacement were similar for the Type 1 and 2 test piles (Figure 5). As the ground surface displacement increased, the horizontal load at the same displacement for the Type 2 pile became larger than that for the Type 1 pile. This result suggests

that the horizontal resistance of the pile increases with the diameter of the soil-cement.

The analytical results for Cases 1-2 and 1-4 were compared with the measured values for the Type 1 pile. Up to a horizontal load of 240 kN, the analytical results for Cases 1-2 and 1-4 showed the same behavior as the measured values for the Type 1 pile. After the gradient of the measured value changed at a horizontal load of 240 kN, Case 1-4 with thin solid elements showed behavior similar to the measured values.

The analytical results for Cases 2-2 and 2-4 were compared with the measured values for the Type 2 pile. Case 2-4 with thin solid elements showed behavior similar to the measured values up to a horizontal load of 240 kN. After the gradient of the measured values changed above a horizontal load of 260 kN, the measured values of the Type 2 pile were between the analytical results for Cases 2-2 and 2-4.

The trends for the Type 1 (Cases 1-2 and 1-4) and 2 analysis results (Cases 2-2 and 2-4) were different. However, Cases 1-4 and 2-4 with thin solid elements showed behavior similar to the measured values of the Type 1 and 2 piles, respectively, compared with Cases 1-2 and 2-2 without thin solid elements. Thus, the behavior of the pile under horizontal load was simulated by modeling the slippage between the H-section steel and soil-cement and between and soil-cement and ground with thin solid elements in the analytical model.

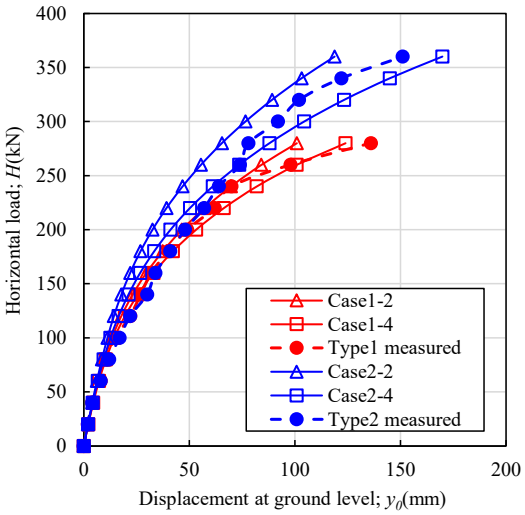

Figure 7. Relationships between horizontal load and displacement at ground level.

4.3 *Bending moment distribution*

The depth distributions of the bending moments for the full-scale horizontal loading tests are shown in Figure 8 and Figure 9. Cases 1-3 and 1-4 and Cases 2-3 and 2-4 are also shown with the test results to demonstrate the effect of the modeling method used for the H-section steel. Cases 1-3 and 2-3 used solid elements for modeling the H-section steel, whereas Cases 1-4 and 2-4 used beam elements. In all cases, thin solid elements were used to simulate slippage between the ground and soil-cement and between the H-section steel and soil-cement. Figure 8 shows the Type 1 pile results and the analysis results (Cases 1-3 and 1-4), and Figure 9 shows the Type 2 pile results and the analysis results (Cases 2-3 and 2-4). The bending moments are shown in panels (a) to (d) for horizontal loads of H = 40, 80, 120, and 240 kN, respectively. The bending moments of the test values were calculated by using only the measured strain of the H-section steel and sectional secondary moment of the H-section steel. Similarly, the bending moments of the analytical results were calculated using the strain of the H-section steel and the Young's modulus and sectional secondary moment of the H-section steel.

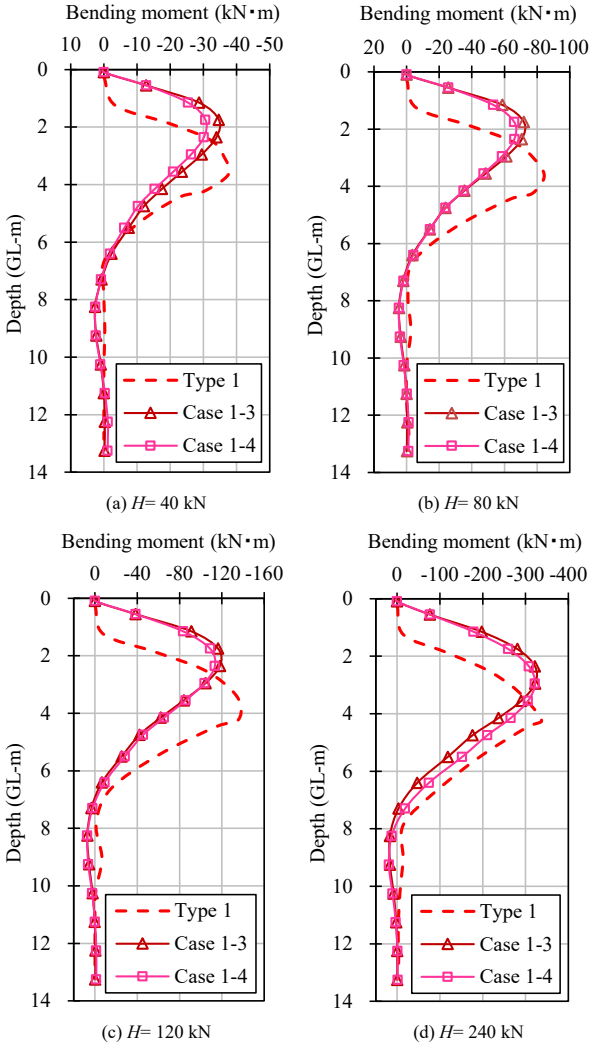

Figure 8. Distribution of the bending moment for the Type 1 pile.

Figure 8 and Figure 9 show that the bending moments were generated mainly up to about GL −6.0 m, and almost none were generated at depths greater than GL −8.0 m. Comparing the measured values of Type 1 in Figure 8 and Type 2 in Figure 9, the maximum bending moment of Type 1 was about 30 kN·m larger than that of Type 2 at a horizontal load of 240 kN. The difference was caused by damage to the soil-cement before the horizontal load of 240 kN was applied, which probably increased the bending moment carried by the H-section steel. Furthermore, the depth at which the maximum bending moment was generated tended to become deeper as the horizontal load increased.

The bending moment distribution of the analysis results were compared with the measured values. In Figure 8 (a), Case 1-3, in which solid elements were used to model the H-section steel, showed a maximum bending moment of about 35 kN·m, which was closer to the measured value than Case 1-4. However, for horizontal loads of H = 80 (Figure 8 (b)) and 120 kN (Figure 8 (c)), no significant differences were observed between Case 1-3 using solid elements and Case 1-4 using beam elements. The maximum bending moment values of the analytical value were about 15 kN·m smaller than the measured values at H = 80 kN, and about 20 kN·m smaller at H = 120 kN. Although no differences were observed between Cases 1-3 and

1-4 in for H = 240 kN (Figure 8 (d)), the maximum bending moment in both cases was about 330 kN·m, which was similar to the measured value. At depths below the maximum bending moment, Case 1-4 shows a bending moment distribution closer to the measured values than Case 1-3. Furthermore, the trend in the analytical results, in which the depth at which the maximum bending moment was generated increased with the horizontal load, was consistent with the measured values. However, for all horizontal loads from Figure 8 (a) to (d), the depth at which the maximum bending moment was generated in the analysis values tended to be shallower than that in the measured values.

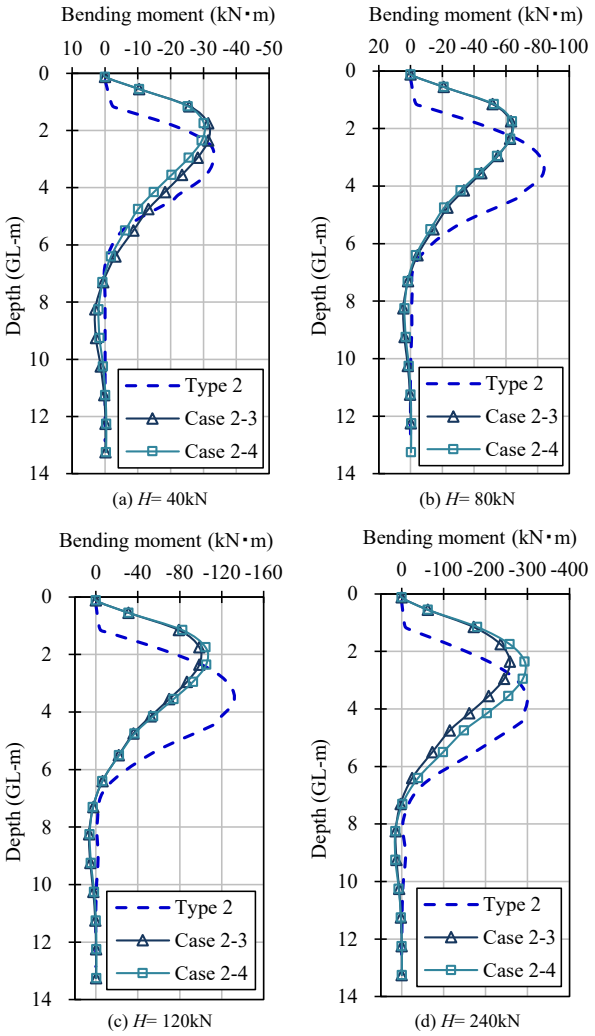

Figure 9. Distribution of the bending moment for the Type 2 pile.

No difference was observed in the bending moment distribution between Cases 2-3 and 2-4 for the small horizontal loads of H = 40 and 80 kN (Figure 9). For H = 40 kN (Figure 9 (a)), the maximum bending moments in both analysis results were similar to that in the measured results. However, for H = 80 kN, the maximum bending moments in both analysis results were about 20 kN·m lower than the measured value (Figure 9 (b)). For a larger horizontal load (H = 120 kN), the maximum bending moment in the analysis results was smaller than the measured value, but the maximum bending moment in Case 2-4, which modeled the H-section steel using beam elements, was about 5% larger than that in Case 2-3 (Figure 9 (c)). For H = 240 kN, the maximum bending moment in Case 2-4 was about 10 kN·m larger than that in Case 2-3 and was similar to the measured maximum bending moment of about 300 kN·m (Figure 9 (d)).

For large horizontal loads of H = 120 and 240 kN (Figure 8 and Figure 9), Case 1-4, which used beam elements in the modeling of the H-section steel, showed a bending moment distribution closer to the measured values than Case 1-3, which used solid elements. However, in all analysis cases, the maximum bending moments were observed at a depth 1 to 2 m shallower than the measured value. Furthermore, the analysis results showed that bending moments were generated at depths of GL −8 to −11 m, which was a different trend from the measured values. These results may have been caused by only evaluating the bending stiffness of H-section steel and calculating the bending moment for the in situ full-scale horizontal load test. In addition, in the analysis, the deformation modulus of the ground at GL −8 to −11 m was greater than that of the field ground, which may have caused the depth at which the maximum bending moment was generated to be shallower than the measured value, and thus generated a bending moment at a deeper position. However, although there was no damage after the compression load test and tensile load test, it is possible that there was some damage to the test pile, which may have affected the horizontal loading test results.

Furthermore, the clearance that was observed on the back of the H-section steel and the shear failure at the flange tip, which were seen in the observations after the horizontal load test (Figure 6), were not simulated in the analysis. The separation and shear failure reduced the stiffness of the upper part of the pile, thereby reducing the bending moment. If soil-cement separation and shear failure can be modeled in the analysis, the increase of the maximum bending moment generating depth with increasing load could be simulated.

5 CONCLUSION

To evaluate the lateral resistance of soil-cement composite piles as permanent piles, we conducted in situ full-scale horizontal loading tests and performed numerical analysis to simulate the loading tests. The following observations were made based on the results of the in situ horizontal loading tests and numerical analysis.

- After the in situ full-scale loading test, clearance between the back of the H-section steel in the loading direction and cracks connecting the flange tips of the H-section steel were observed. This result suggested that in the process of reaching the maximum horizontal load, tensile forces at the boundary between the soil-cement and H-section steel caused the separation, which then induced shear failure at the tip of the H-section steel flange.
- The analysis cases with thin solid elements obtained results that were closer to the measured values compared with the analysis cases without thin solid elements for the relationships between horizontal load and displacement at ground level. Thus, the behavior of the pile under horizontal load was simulated by modeling the slippage between the H-section steel and soil-cement and between and soil-cement and ground with thin solid elements in the analytical model.
- According to the bending moment distribution, the analysis cases that used a beam element for modeling the H-section steel showed a maximum bending moment closer to the measured values compared with the analysis cases that used a solid element for modeling the H-section steel.
- The modeling using thin solid elements was suitable for simulating slippage of the ground and soil-cement and the soil-cement and H-section steel. In addition, the modeling by the beam element for the H-section steel was suitable

for simulating the bending behavior of the soil-cement composite pile.

- In the numerical analysis, the accuracy of the bending moment distribution was improved by evaluating the bending stiffness of the piles, including soil-cement, and revising the deformation modulus of the ground. Furthermore, evaluating the delamination of the soil-cement and H-section steel, the shear failure of the soil-cement, and the resulting decrease in pile stiffness are challenges highlighted by this study.

6 REFERENCES

Japanese Geotechnical Society, 2010. *Standards of the Japanese Geotechnical Society (Method for Lateral Load Test of Piles)* (in Japanese). Japan: Japanese Geotechnical Society

Japanese Society of Soil Mechanics and Foundation Engineering, 1982. *Handbook of soil mechanics and foundation engineering*. Japan: Japanese Society of Soil Mechanics and Foundation Engineering

Kitaura, M., Kohono, T., Nishida, H., Nanazawa, T., Nakatani, S., Tokoyama, M., Yoshikawa, N., Tsuda, K. 2014. Bearing capacity characteristic after lager deformation of actual piles constructed by pre-boring, *Jornal of Japan Society of Civil Engineers, Ser.C (Geosphere Engineering)*, Vol.70, pp. 106-124 (in Japanese).

Koga, K., Watanabe, K. & Yamamoto, T. 2022. Study on vertical bearing characteristics for soil-cement composite pile. *Journal of structural engineering. A*, Vol. 68A, pp. 158-169 (in Japanese).

Railway Technical Research Institute. 2001. *Design Standard for Railway Structures and Commentary (Cut and Cover Tunnel)*. Japan: Maruzen Publishing Co., Ltd.

Railway Technical Research Institute. 2012. *Design Standard for Railway Structures and Commentary (Foundation Structures)*. Japan: Maruzen Publishing Co., Ltd.